

Modeling of Fiber-Reinforced Elastomeric Base Isolators



Animesh Das

Research Scholar, Civil Engng. Deptt., IIT Guwahati

Anjan Dutta

Professor, Civil Engng. Deptt., IIT Guwahati

S.K. Deb

Professor, Civil Engng. Deptt., IIT Guwahati

SUMMARY:

Finite element simulations were carried out using ANSYS for the mechanical characterization of multi-layer elastomeric isolation bearings where the reinforcement elements were fiber reinforced plastic instead of conventional steel plates. Fiber reinforced elastomeric isolation bearings are low cost alternative to the conventional steel-reinforced bearings. Some experiments were conducted in the past to assess their effectiveness. Validating the results by numerical modeling would allow analysis of bearings when it would not be possible to do so experimentally. The development of lightweight, low-cost isolator is crucial if this method of seismic protection is to be applied to a wide range of buildings such as residential, school and hospital buildings etc. in rural and urban earthquake-prone zones.

Thus, circular and a rectangular isolator models were attempted for the analysis. Horizontal displacements were applied at different strain levels and the horizontal stiffness and damping ratios were calculated. Further, comparisons were made between bonded and un-bonded FRP isolators and their performance when subjected to loading in different directions.

Keywords: Base Isolator, FRP, Un-bonded, Finite Element.

1. INTRODUCTION

In passive seismic protection systems, base isolation plays an important role. It is an efficient and viable method to reduce the vulnerability of structures in high seismic risk zones. Currently this technique is limited only to large, expensive buildings housing sensitive instruments and hospitals. In developing countries like India even this is rare. This is because the isolators used for such structures are quite expensive. This makes them very uneconomical to use in housing, schools and even in commercial buildings. To make the base isolation a viable method in such buildings, it is necessary to reduce the cost of the isolators.

Conventionally, steel plates are used as reinforcing material. Its function is to provide vertical stiffness to the isolator to take the weight of the structure. Bearings using steel as reinforcing material are known as steel-reinforced elastomeric bearings (SREI). Thin sheets of steel are interspersed in between layers of rubber. However, steel reinforcement has some disadvantages. Steel is heavy and makes up for most of the weight of the isolator. Further, thick end-plates are needed on both ends of the isolators which adds to the total cost. The process of bonding steel with the rubber involves placing steel plates between rubber layers and heating them under pressure for several hours. The entire process is complicated and expensive. All these make conventional isolators unsuitable for use in smaller and less important buildings, particularly in developing and under-developed countries. This problem can be overcome by using an alternative to steel, which has stiffness comparable to that of steel but is lighter and less expensive to manufacture.

Many fiber materials whose stiffness is comparable to steel are now available. Seismic isolators can be designed using layers of rubber, bonded with thin layers of bidirectional fiber fabric (Kelly and Takhirov 2001). Replacing steel with fiber, isolators of much lesser weight can be manufactured. Bearings with fiber reinforcement and elastomeric damping material are called fiber-reinforced

elastomeric isolator (FREI) bearings. Additional benefits are obtained in the form of considerable reduction in the manufacturing costs resulting from a lesser labour – intensive process. It is also possible to reduce the costs further by replacing the current bonding process by microwave heating in an autoclave which is cheaper.

Lateral response characteristic of square FREI were studied by Toopchi-Nezhad et. al. 2008. Bearings were manufactured with neoprene compound as the elastomer and carbon fiber fabric as reinforcement. An un-bonded test, where bearing ends were not connected to the test machine by end plates were performed. Stable roll over deformations were observed in the bearing, which reduced the effective lateral stiffness of bearing. In case of un-bonded isolators subjected to lateral displacement, separation was observed along the trailing edge of the bearing and the base support as well as between the loading edges of the bearing and the superstructure. Properly designed un-bonded FREI bearings exhibit larger lateral displacement capacity compared to the same bearing in bonded form. Test result revealed that lateral load displacement hysteresis behavior was comparable to that of conventional steel reinforced bearings. The test performed according to ASCE provision, concluded that the FREI bearings may be used for un-bonded application for low rise buildings having fixed base time period of around 0.2 second.

Conventionally base isolation systems are designed to be isotropic and base isolators are always considered to be symmetric. So, the isolators being manufactured currently are either circular or square in shape. Fiber-reinforced isolators can be easily cut to required shape and size which is not possible with steel reinforced isolators. Another benefit of using fiber reinforcement is that it stretches under loading and is very flexible in bending. The steel reinforcement is assumed to be inextensible and rigid in flexure. Fiber reinforcement consists of cords which are made from individual fibers grouped and coiled together (Kelly and Takhirov 2001). These cords are more flexible in tension compared to individual fibers causing them to stretch under loading. During shear loading of these cords, plane cross sections become curved. The tension in the cords, acting on the curvature of the reinforcing sheet causes individual strands to slip resulting in frictional damping. This provides additional damping in the isolator. Tsai and Kelly 2001 theoretically analyzed the compressive stiffness and bending stiffness of fiber-reinforced isolators having three types of geometry: infinitely long strip, rectangular and circular. They derived the stiffness formulae of fiber-reinforced isolators, studied the effect of fiber flexibility on its mechanical properties and showed that it was theoretically possible to design fiber-reinforced isolators with properties comparable to those of steel-reinforced isolators. Kelly and Takhirov 2002 conducted experiments on circular un-bonded fiber-reinforced bearings. Two types of tests were conducted on the bearings. The first was a vertical load test wherein the vertical load was gradually applied and varied and the corresponding stiffness and compressive modulus of the bearing were calculated. In the second test, a constant vertical pressure was applied and varying horizontal displacement was applied. The resulting lateral stress vs strain graph was plotted. Then they calculated the lateral stiffness and the damping of the isolator. The strain level and the vertical pressure applied were varied and the variations in damping as well as lateral stiffness were studied. Moon et. al. 2002 fabricated fiber reinforced elastomeric isolator bearings and carried out experiments under vertical and horizontal loading conditions. They also tested steel reinforced elastomeric isolators and compared the performance of these isolators to the performance of the FREIs. Hamid et. al. 2008 studied the experimentally obtained lateral response characteristics of scaled square un-bonded fiber-reinforced elastomeric isolator. ¼ scale carbon-fiber bearings with soft unfilled neoprene as the damper were used in their experiment. Horizontal load was applied at angles of 0°, 45° and 90° to the reference plane. Experimentally obtained result of lateral load – displacement hysteresis loops of the FREI with un-bonded application were observed to be comparable to the conventional steel reinforced bearings. Toopchi-Nezhad et. al. 2011 carried out finite element analysis of FREI and validated the same with experimental observations.

It has been observed that the FREI bearings have mechanical properties comparable to conventional steel-reinforced bearings. However, the experimental study was mostly carried out on orthodox shapes (circular and square). It is not possible to experimentally analyze bearings of all shapes and sizes. This necessitated finite-element modeling of FREI bearings, where there would be no restriction on the shape and size of the bearing.

The objective of this study was to verify the feasibility of fiber-reinforced elastomeric base isolators as a viable alternative to the conventional steel-reinforced isolators through finite element modeling of

the isolators. The performances of different types of isolators under different loading conditions were studied. Two different rectangular isolators were modeled and analyzed. One was having relatively high length to breadth ratio and acted like a long strip isolator, while the other one was with lesser length to breadth ratio. The circular isolator and both the rectangular isolator were analysed for horizontal cyclic displacement of different amplitudes. From the result of cyclic displacement analysis, effective horizontal stiffness and damping of the isolator were obtained. The results were further analysed to study the performance of un-bonded isolators in comparison with bonded isolators. Moreover, results of different types of isolator were also compared to ascertain the performances of various types for different application areas.

2. FINITE ELEMENT METHOD

To analyze the mechanical properties of FREI bearings, finite-element modeling was done. The isolator was modeled using ANSYS12.1 Multi-physics finite-element software. The software has integrated pre and post-processing facilities, capability for robust static and dynamic structural analysis (both linear and non-linear) and has large element and material library. Three isolators, one circular and two rectangular were modeled and analyzed. The circular isolator was analyzed as both bonded and un-bonded cases, while the rectangular isolators were analyzed for un-bonded case. As the conventional isolators are bonded, the comparison of bonded and un-bonded isolators provided information about the advantages gained by using fiber reinforced un-bonded isolators.

2.1. Element Types

Each layer of fiber-reinforcement was made up of thin layers of bidirectional (0/90 orientation) carbon fiber fabric. The thickness of each fiber was 0.3mm. SOLID46, a 8-node layered structural solid was used to model the reinforcement. The element has three translational degrees of freedom at each node along x, y, and z directions. The end plates were modeled using SOLID185, a 8-node structural solid element. A very high elastic modulus was used to keep the end plates relatively rigid. The elastomer used was neoprene rubber and was modeled using SOLID185.

Further, in un-bonded case, the isolator was not attached to the end plates. During lateral loading, separation occurred between the top surface of the isolator and the top plate as well as the bottom surface of the isolator and the bottom plate. Using disjointed models for the isolator and the end-plates, the analysis would be erroneous as the transfer of load would not take place and the elements would behave independent of each other. Hence contact elements were introduced to model the isolator-plate interfaces. This modeling was done using 3-D surface-to-surface contact elements CONTA173 and TARGE170. Rough contact surface was used as the shear force was to be transferred from the end plate to the isolator. Contact elements are non-linear and their solving requires lot of computational power.

2.2. Material Properties

The fiber reinforcement was modeled as a linear orthotropic element with the following properties as available in standard literature:

$$E_x = 4.4 \times 10^{10} \text{ Pa} ; E_y = 4.4 \times 10^{10} \text{ Pa} ; E_z = 1 \times 10^{10} \text{ Pa}$$

$$\nu_{xy} = 0.3 ; \nu_{yz} = 0.25 ; \nu_{zx} = 0.25$$

$$G_{xy} = 1 \times 10^{10} \text{ Pa} ; G_{yz} = 5 \times 10^9 \text{ Pa} ; G_{zx} = 5 \times 10^9 \text{ Pa}$$

Elastomer was modeled with hyperelastic and viscoelastic parameters. Hyperelasticity refers to materials which can experience large elastic strain that is recoverable. Rubber-like and many other polymer materials fall in this category. The constitutive behavior of hyperelastic materials are usually derived from the strain energy potentials. Further, hyperelastic materials generally have very small compressibility. This is often referred to as incompressibility. Hyperelastic materials have a stiffness

that varies with the stress level. Ogden 3-terms model was adopted to model the hyperelastic behavior of the rubber and the viscoelastic behavior was modeled by Prony Viscoelastic Shear Response parameters. The material parameters used were:

$$\text{Ogden (3-terms)} \quad \mu_1 = 1.89 \times 10^6; \mu_2 = 3600; \mu_3 = -30000$$

$$\alpha_1 = 1.3; \alpha_2 = 5; \alpha_3 = -2$$

$$\text{Prony Shear Response} \quad a1 = 0.3333; t1 = 0.4; a2 = 0.3333; t2 = 0.2$$

2.3. Geometrical Properties

To carry out finite element analysis of circular isolator, the geometry of isolator is chosen from Kelly and Takhirov 2001. Geometrical properties of circular isolator are listed in Table 2.1. For rectangular, the geometry of isolator is chosen from Kelly and Takhirov 2002. Geometrical properties of rectangular isolator are listed in Table 2.2.

Table 2.1 Geometry of Circular Isolator

Circular Isolator	
Diameter	305 mm
Total height	141 mm
Thickness of fibre layer	3 mm
Number of fibre layer	13
Thickness of rubber layer	8.5 mm
Number of rubber layer	12
Bonded end plate diameter	305 mm
Un-bonded end plate	340 mm
Un Un-bonded end plate thickness (Top and bottom)	15 mm

Table 2.2 Geometry of Rectangular Isolator

Rectangular Isolator	Isolator 1	Isolator 2
Length	750 mm	375 mm
Width	190 mm	190 mm
Total height	120 mm	120 mm
Thickness of fibre layer	1.8 mm	1.8 mm
Number of fibre layer	11	11
Thickness of rubber layer	10 mm	10 mm
Number rubber layer	10	10
Length of end plate	800 mm	420 mm
Width of end plate	240 mm	240 mm
Thickness of end plate	15 mm	15 mm

2.4. Meshing

The models were meshed with hexagonal volume sweep. The volume sweep fills existing unmeshed volume with elements by sweeping the mesh from an adjacent area through the volume. If the area is not already meshed, volume sweep meshes the area and then extrudes it. Fig. 2.1-2.4 show finite element meshes for all the isolators considered in the present study.

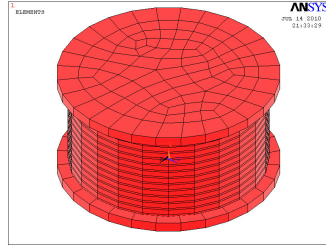


Figure 2.1. Meshed Circular unbounded Isolator

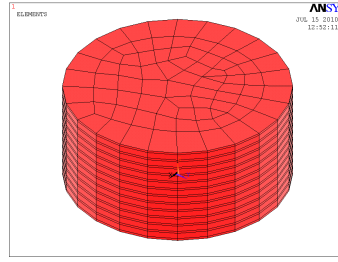


Figure 2.2. Meshed Circular bounded Isolator

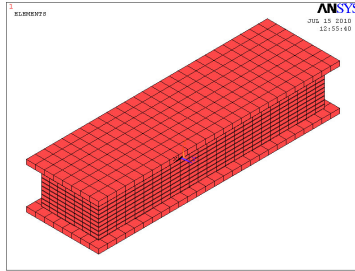


Figure 2.3. Meshed Rectangular Isolator 1

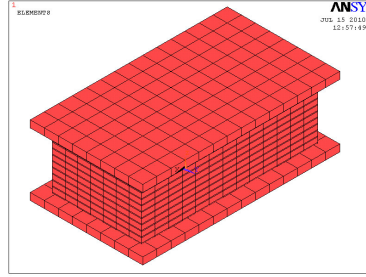


Figure 2.4. Meshed Rectangular Isolator 2

3.1 ANALYSIS FOR HORIZONTAL LOAD

A constant vertical load was applied on the isolator and cyclic horizontal displacements of different amplitudes were applied at the top of isolator. The applied vertical load was 6.9MPa (Kelly and Takhirov 2001) for circular and Rectangular isolator 1 and 3.45MPa (Kelly and Takhirov 2002) for the Rectangular isolator 2. For rectangular isolators, the horizontal displacement was applied at 0°, 45° and 90° to the longer dimension. Maximum horizontal displacements applied were 50%, 100% and 150% of rubber thickness. A typical horizontal displacement history is shown in Fig.3.1. Transient dynamic analysis was carried out to analyze the bearings. The full method was used which utilizes the full system matrices to calculate the transient response. It is the most general of the three methods because it allows all types of nonlinearities to be included (plasticity, large deflections, large strain, and so on). The results obtained are the most accurate among the various methods. Full method was used in case of analyzing the bearings because of the material non-linearity, non-linearity of the contact element and also the varying time steps. Displacement based convergence criteria was used for the analysis under horizontal load.

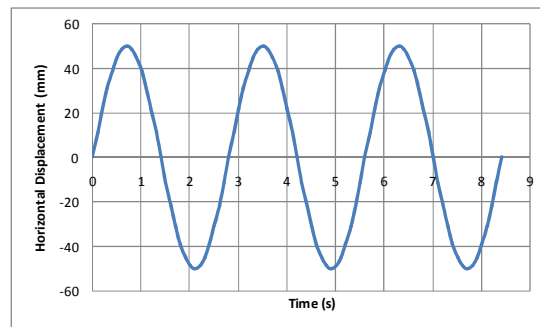


Figure 3.1. Imposed horizontal displacement history at 50mm displacement

4. RESULTS AND DISCUSSION

The total force in the loading direction on all the nodes at the top surface are summed to get the total shear force. The shear force is then plotted against the applied horizontal displacement. The plots obtained were analyzed to obtain the effective horizontal stiffness (K_{eff}^h) and damping ratio (β).

$$K_{eff}^h = (F_{max} - F_{min}) / (d_{max} - d_{min}) \quad (4.1)$$

where, F_{max} is maximum value of shear force

F_{min} is minimum value of shear force

d_{max} is maximum value of displacement

d_{min} is minimum value of displacement

The hysteresis loops were analyzed to obtain the equivalent viscous damping ratio (β) of the isolators for different loading cases. The area contained in the hysteresis loop in force vs displacement curve gives the energy dissipated. The damping ratio was calculated as

$$\beta = W_d / (4\pi W_s) \quad (4.2)$$

where, W_d is the dissipated energy and evaluated as the area under hysteretic loop

W_s is elastic energy and is written as

$$W_s = (K_{eff}^h (\Delta_{max})^2) / 2 \quad (4.3)$$

Δ_{max} is average of positive and negative maximum displacement and expressed as

$$\Delta_{max} = (d_{max} + |d_{min}|) / 2 \quad (4.4)$$

4.1. Circular Isolator

Vertical load vs the vertical displacement is shown in Fig.4.1. The vertical stiffness, K_v , of the isolator was evaluated as 1513MN/m. Bearings of the same dimensions were tested at the University of California at Berkeley. The bearings were handmade and showed some design imperfections which could be seen in the scatter in the vertical stiffness. Hence the vertical stiffness was much lower about 340 MN/m (Kelly and Takhirov 2001).

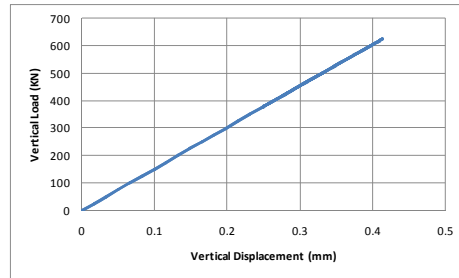


Figure 4.1. Vertical load vs vertical displacement

Fig. 4.2 and 4.3 show the load –displacement curves for circular isolators along with typical deformed configuration of isolators. The detailed results are given in Table 4.1. It was observed that in both bonded and un-bonded cases, the horizontal stiffness reduced with increase in the maximum displacement. However, while the lateral response of the bonded one remained nearly linear, the un-bonded behaved nonlinearly due to the rollover deformation. As a result of the rollover deformation, the horizontal effective secant stiffness decreased with increased lateral displacement. For a given

maximum displacement, the horizontal stiffness was higher for the bonded isolator as compared to the un-bonded isolator. The difference in stiffness was lesser for smaller displacements but was more noticeable at higher displacements. At 50mm displacement, about 1.6% difference in stiffness between bonded and un-bonded was observed, while the same was as high as about 12.6% at 150mm displacement. This is because for the un-bonded case at smaller displacements, the contact between the end plates and the isolator was not lost and hence showed stiffness values close to the bonded isolator. However, as the imposed horizontal displacement increased for un-bonded isolator case, the separation of end-plates and isolator became significant and caused reduction in stiffness. The horizontal stiffness values of the un-bonded isolator are comparable to those obtained experimentally at the University of California at Berkeley (UCB) for higher displacement. However, for lower value of displacement, the horizontal stiffness is observed to vary significantly with the test result of UCB (Kelly and Takhirov 2001).

In both the cases, the damping values increased with increase in the maximum displacement. This increase was however more significant at lower displacements as compared to those at higher displacements. The damping ratio of un-bonded isolator was slightly higher than the bonded isolator. The difference was noticeable only at higher displacements as was also observed for horizontal stiffness.

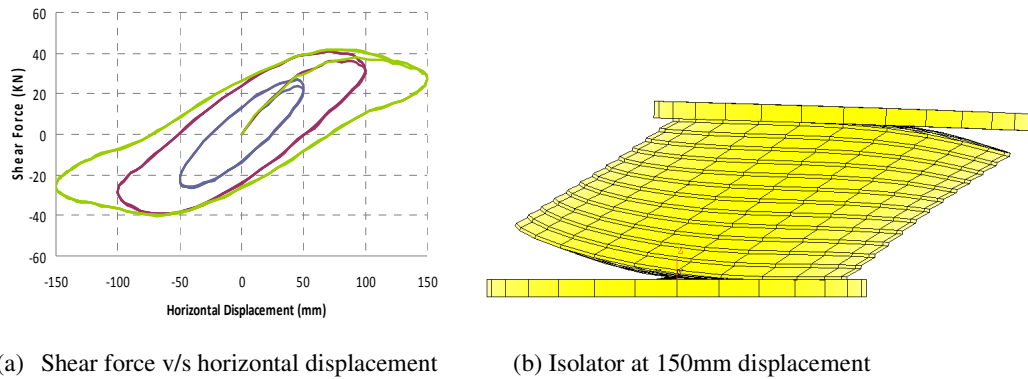


Figure 4.2. Un-bonded circular isolator

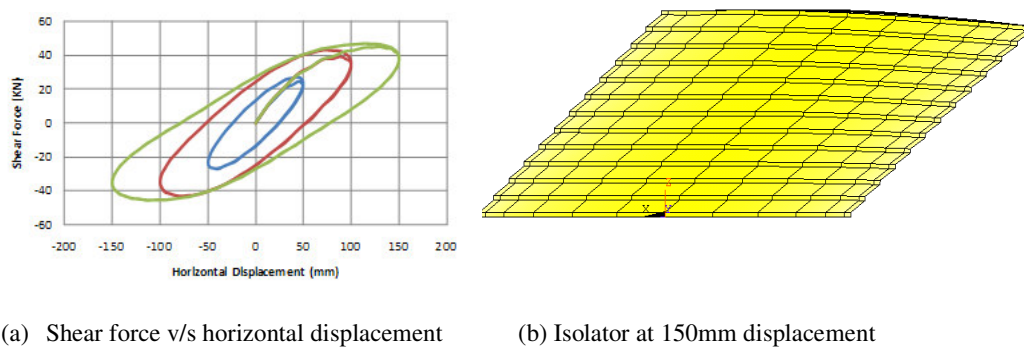


Figure 4.3. Bonded circular isolator

Table 4.1 Horizontal Response of Circular Isolator

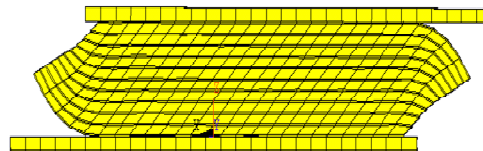
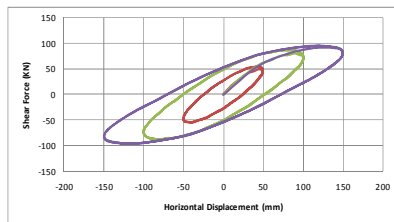
Maximum Displacement (mm)	Un-bonded Circular Isolator		Bonded Circular Isolator	
	K_{eff}^h (kN/m)	Damping (%)	K_{eff}^h (kN/m)	Damping (%)
50	536	24.4	545	24.2
100	411	27.4	433	27.1
150	278	28.0	313	27.5

4.2. Rectangular Isolator

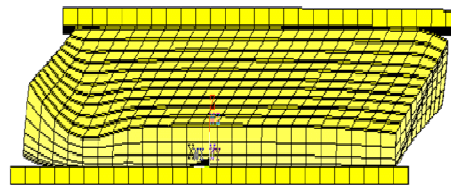
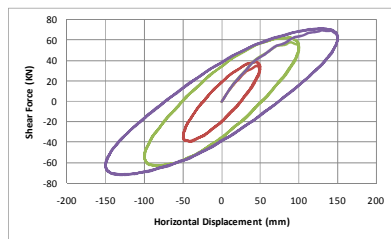
Fig. 4.4 and 4.5 show the load – displacement curves for different rectangular isolators loaded along different directions along with typical deformed configuration of isolators. Stable rollover deformations were observed at higher displacement in both the cases. The detailed results are given in Table 4.2. It may be noted that the direction 0° indicates the applied displacement is along the longitudinal direction of isolator and 90° indicates the applied displacement is along the shorter direction of isolator. The horizontal stiffness of the Rectangular isolator 1 was observed to be higher than that of the Rectangular isolator 2. The ratio of their stiffness is around 2, which corresponds to the ratio of their loaded surface areas (top surfaces). For both of the isolator, the horizontal stiffness was higher at lower displacement and decreased with the increase in displacement in the direction of loading. The damping values were observed to be lower at lower displacement and higher at higher displacement for both the isolators.

Shear force v/s horizontal displacement

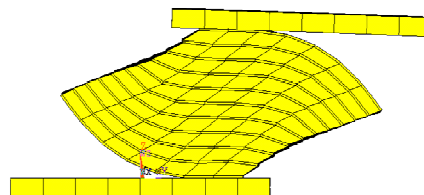
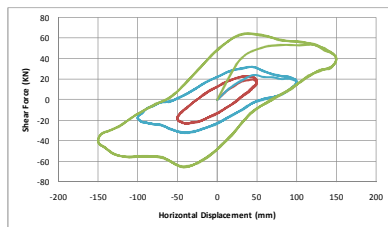
Isolator at 150mm displacement



(a) at 0° loading



(b) at 45° loading

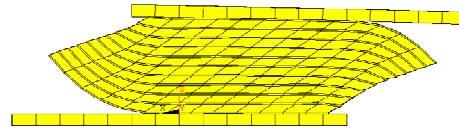
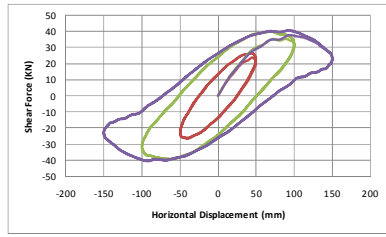


(c) at 90° loading

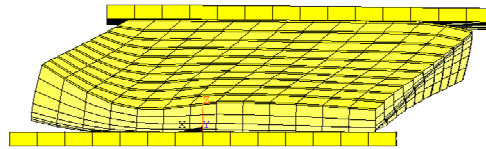
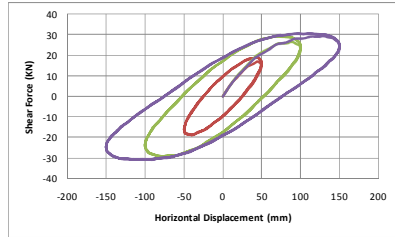
Figure 4.4. Rectangular Isolator 1

Shear force v/s horizontal displacement

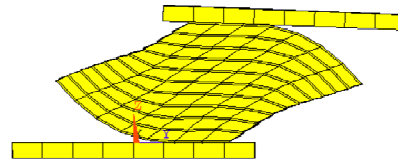
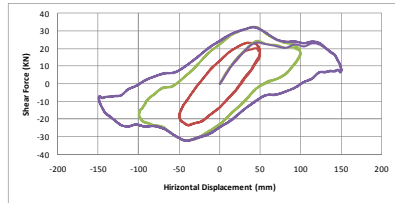
Isolator at 150mm displacement



(a) at 0° loading



(b) at 45° loading



(c) at 90° loading

Figure 4.5. Rectangular Isolator 2

Table 4.2 Horizontal Response of Rectangular Isolator

Loading direction	Maximum Displacement (mm)	Rectangular Isolator 1		Rectangular Isolator 2	
		K_{eff}^h (kN/m)	Damping (%)	K_{eff}^h (kN/m)	Damping (%)
0°	50	1096	24.1	531	24.9
45°	50	780	24.2	458	24.8
90°	50	457	27.4	376	27.4
0°	100	865	27.0	398	28.1
45°	100	629	26.6	323	27.9
90°	100	421	29.7	293	29.6
0°	150	643	26.2	271	28.0
45°	150	478	25.6	214	28.6
90°	150	323	28.1	205	29.1

4.3. Comparison among Isolators

The circular isolator and the shorter rectangular isolator were of about the same area. Though shapes were different, the total rubber layer thickness was almost same (102mm and 100mm respectively) and hence their performance in the horizontal direction could be observed as comparable. The horizontal stiffness of the circular isolator was marginally higher than that of the rectangular isolator 2 for 0° loading case. In other direction of loading, the horizontal stiffness of rectangular isolator 2 was however much lesser than that of circular isolator. This shows that circular isolators can be replaced by rectangular isolators of same area without significant reduction in performance. Similarly, both the rectangular isolators showed similar stiffness at lower displacement for 0° loading case. The values however differed at higher displacement. Thus, rectangular strips of isolators can be introduced in masonry building, where the size of rectangular isolator can be chosen depending on the horizontal stiffness requirement.

5. CONCLUSION

The numerical simulation of FREI using ANSYS, general purpose finite element software showed very consistent behavior of different types of isolators considered in the present study. Thus, the numerical modeling can be seen as an alternative to quite involved experimental studies of base isolators.

The un-bonded isolators showed stable rollover deformed shape at higher displacement and hence would be very effective in seismic isolation of buildings mounted on the top of such isolators. Studies on different shapes showed the usefulness of any desired shape with appropriate dimension to suit specific requirements. Further, while the horizontal stiffness values are comparable to those of conventional isolators, higher damping makes FREIs as even better choice.

REFERENCES

- Kelly, J. M. and Takhirov, S. M. (2001). Analytical and Experimental Study of Fiber-Reinforced Elastomeric Isolator. *PEERR Report*, 2001/11.
- Kelly, J. M. and Takhirov, S. M. (2002). Analytical and Experimental Study of Fiber-Reinforced Strip Isolators. *PEERR Report*, 2002/11.
- Moon, B.Y, Kang, G. Ju, Kang B. Soo and Kelly, J.M. (2002). Design and Manufacturing of Fiber Reinforced Elastomeric Isolator for Seismic Isolation. *Journal of Material Processing Technology* **130-131**, 145-150.
- Tsai, Hsiang-Chuan and Kelly, J. M. (2001). Stiffness Analysis of Fiber-Reinforced Rectangular Seismic Isolator. *Journal of Engineering Mechanics, ASCE* **128:4**, 462-470.
- Toopchi-Nezhad, H., Tait, M.J. and Robert, G. (2011). Bonded versus un-bonded strip fiber reinforced elastomeric isolators: Finite element analysis, *Composite Structures* **93**, 850–859.
- Toopchi-Nezhad, H., Tait, M.J. and Drysdale, R.G. (2008). Testing and modeling of square carbon fiber-reinforced elastomeric seismic isolators. *Struct Control Health Monitoring* **15:6**,876–900.